Atmos. Chem. Phys., 12, 4399–4411, 2012
www.atmos-chem-phys.net/12/4399/2012/
doi:10.5194/acp-12-4399-2012

Atmospheric Chemistry and Physics

Sulfuric acid nucleation: power dependencies, variation with relative humidity, and effect of bases

J. H. Zollner[1], W. A. Glasoe[1], B. Panta[1], K. K. Carlson[1], P. H. McMurry[2], and D. R. Hanson[1]

[1]Department of Chemistry, Augsburg College, Minneapolis, MN 55454, USA
[2]Department of Mechanical Engineering, University of Minnesota, Minneapolis, MN 55455, USA

Correspondence to: D. R. Hanson (hansondr@augsburg.edu)

Received: 16 December 2011 – Published in Atmos. Chem. Phys. Discuss.: 12 January 2012
Revised: 6 April 2012 – Accepted: 3 May 2012 – Published: 16 May 2012

Abstract. Nucleation of particles composed of sulfuric acid, water, and nitrogen base molecules was studied using a continuous flow reactor. The particles formed from these vapors were detected with an ultrafine condensation particle counter, while vapors of sulfuric acid and nitrogen bases were detected by chemical ionization mass spectrometry. Variation of particle numbers with sulfuric acid concentration yielded a power dependency on sulfuric acid of 5 ± 1 for relative humidities of 14–68 % at 296 K; similar experiments with varying water content yielded power dependencies on H_2O of $\sim$7. The critical cluster contains about 5 H_2SO_4 molecules and a new treatment of the power dependency for H_2O suggests about 12 H_2O molecules for these conditions. Addition of 2-to-45 pptv of ammonia or methyl amine resulted in up to millions of times more particles than in the absence of these compounds. Particle detection capabilities, sulfuric acid and nitrogen base detection, wall losses, and the extent of particle growth are discussed. Results are compared to previous laboratory nucleation studies and they are also discussed in terms of atmospheric nucleation scenarios.

1 Introduction

The origin and abundance of particles in the atmosphere have long been studied due to their potential impact on human health and global climate change (IPCC, 2007; Oberdorster et al., 1992; Nel, 2005). The vast array of condensable molecules in the environment, ranging from abundant species such as water vapor to trace species such as ammonia, sulfuric acid, and organic acids, complicates the study of atmospheric nucleation. Even in laboratory settings the precise role these species play in nucleation of particles has proven difficult to decipher. Consequently, research in this area is ongoing – laboratory nucleation studies involving H_2SO_4 is the subject of this paper.

Many experiments have been performed within the H_2SO_4 and H_2O system where nucleation rates J and their dependency on sulfuric acid concentration and relative humidity (RH) have been explored. Dependencies on reactant concentrations (which are proportional to activities for typical conditions) is important because theory shows that the molecules present in the so-called critical cluster, i.e., the direct precursor to nascent particles, can be inferred from these dependencies (Oxtoby and Kaschiev, 1994; McGraw and Wu, 2003). Ball et al. (1999) in experiments with RH = 5-to-15 % determined power dependencies for sulfuric acid of $\sim$8 while earlier work had power dependencies of 15 (RH = 9, 14 %, Wyslouzil et al., 1991) and 10-to-20 (Viisanen et al., 1997, RH = 38 and 52 %). Zhang et al. (2004) report a power dependency of 8 for sulfuric acid at 5 % RH. More recent work explored nucleation over a wide range of relative humidities. Benson et al. (2008) report sulfuric acid power dependencies between 2 and 10 with larger values occurring at lower RH and Young et al. (2008) report values of 4–8 at 15 % RH and 3 at 23 % RH. Brus et al. (2010) report power dependencies of 4 to 8 on sulfuric acid for experiments at 10, 30, and 50 % RH, i.e., with larger values at higher RH. In later experiments, they report $\sim$1.5 for comparable RH, attributing the difference to improved particle and H_2SO_4 detection (Brus et al., 2011). A number of experiments have explored nucleation at low sulfuric acid levels, $\sim 10^7$ cm^{-3} vs. 10^8-to-10^{10} cm^{-3} in the above studies. Berndt et al. (2005, 2006) report measured nucleation rates that follow power

dependencies of 3 to 5 at RH of 11 to 50 % but more recently Berndt et al. (2010) and Sipila et al. (2010) report power dependencies of 1.5 to 2 on sulfuric acid over a range of 10–50 % RH. However, recent results (Kirkby et al., 2011) at comparable sulfuric acid levels and similar particle counters show a power dependency of ∼6.

McMurry et al. (2000), Kulmala et al. (2004), and Kuang et al. (2010), have shown that empirical nucleation theories can explain observed boundary-layer atmospheric nucleation rates, one theory with J dependent on sulfuric acid with a power dependency of 1 and the other with 2. These observations diverge from classical nucleation theory (Doyle, 1961; Reiss, 1950; Laaksonen et al., 1995; Bein and Wexler, 2007) for neat H_2SO_4/H_2O that predicts power dependencies of 10-to-15 at the $[H_2SO_4]$ found in the atmosphere. This is generally taken as evidence that the observations are dominated by nucleation processes other than the neat H_2SO_4/H_2O system, with ammonia or amines in ternary systems as likely candidates (Weber et al., 1998). Recently, ammonia and amines have been shown to have dramatic effects on J when added to H_2SO_4 and H_2O vapors (Coffman and Hegg, 1995; Ball et al., 1999; Benson et al., 2009; Erupe et al., 2010; Kirkby et al., 2011). Understanding the effect of a third species requires good knowledge of the system being affected: that of nucleation with two species (i.e., neat H_2SO_4-H_2O.)

Described here are experiments on particle formation based on the Ball et al. (1999) techniques. They were conducted over a wide range of relative humidity and sulfuric acid concentration at a constant temperature. The results provide more measurements of nucleation within the H_2SO_4-H_2O system with gas-phase analysis of potential nitrogen base contaminants. Observed particle count rates are analyzed in terms of power dependencies to obtain critical cluster compositions. Experimental issues concerning particle detection (see e.g., Sipila et al., 2010; Berndt et al., 2010) that can complicate the interpretation of flow reactor nucleation experiments are discussed. Also, ammonia and methyl amine were added to assess their relative enhancing effects on nucleation within the neat H_2SO_4-H_2O system.

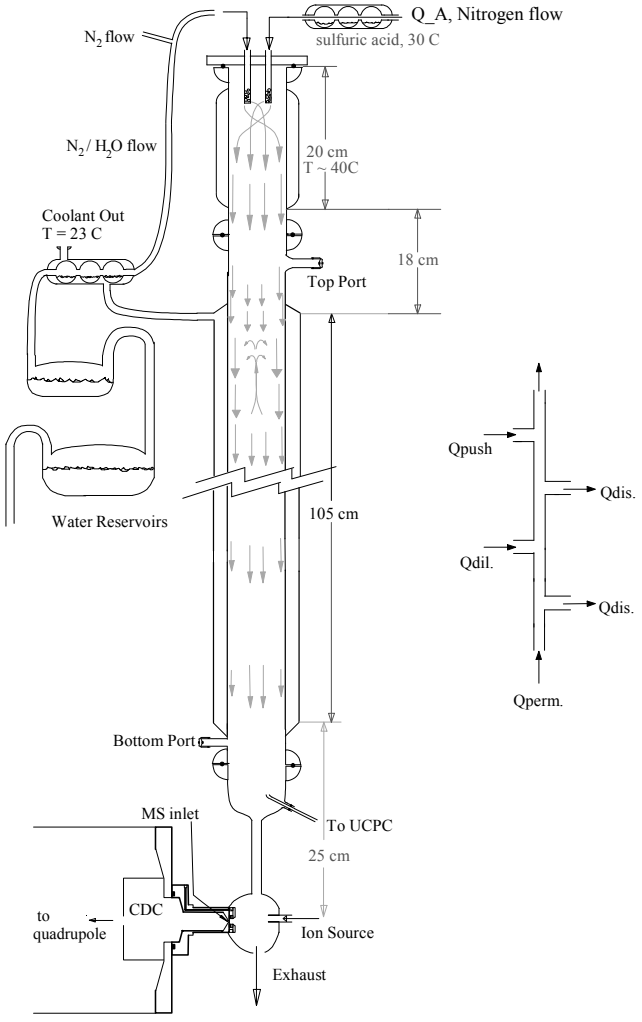

Fig. 1. Schematic drawing of the nucleation flow reactor with mixing region, transition and nucleation regions indicated. Water and H_2SO_4 sources (i.e., the reservoirs), the general flow patterns and temperatures are indicated. Top and bottom ports show where N bases could be added to the flow. The region of highest particle formation rates within the nucleation region are about 30 cm into the cooled region. The dynamic dilution system for adding N bases is shown to the side.

2 Experimental

Similarly to Ball et al., experiments were carried out in a 5 cm inner diameter glass flow reactor (Fig. 1 is a schematic of the reactor) with an overall length of 150 cm. Sulfuric acid was detected with chemical ionization mass spectrometry, and particles were detected with an ultrafine condensation particle counter (UCPC). The following presents an overview of the apparatus and technique.

The top of the vertically-aligned flow reactor serves as a mixing region where gases laden with H_2SO_4 and H_2O vapor mix at a temperature of 313 K (about 20 cm long and 5 cm ID). The mixing region is capped with a manifold (Teflon) for the nitrogen carrier gas + reactant lines. A 50 mm o-ring joint at the top of the mixing region seals to the manifold with a Viton o-ring encapsulated with PTFE. See the Supplement for results of tests where the mixing region temperature was varied. Following the mixing region is the nucleation region, a ∼120 cm long glass flow reactor where particle nucleation and growth occurs. A 105 cm length of it is surrounded by a cooling jacket maintained at 296 K. The interface between the mixing region and the nucleation region is ∼18 cm long, is at room temperature, and the 50 mm o-ring joint is also sealed with a PTFE encapsulated Viton o-ring.

The total carrier N_2 flow was 6 sLpm (l min^{-1} at STP: 273 K, 1 atm) which results in an average carrier flow speed

of $\sim$6 cm s^{-1} for typical conditions of 0.98 atm and 296 K. N_2 was taken from a liquid nitrogen gas pack, i.e., vapor from liquid nitrogen, which is essentially free of condensable contaminants. To enhance the cleanliness of the flow reactor by minimizing its exposure to room air, a flow of nitrogen ($\sim$ 1 sLpm) was left on between experiments continuously now for over a year.

Water was introduced to the system by directing a portion of the carrier nitrogen over one or two water reservoirs in series at room temperature for initial humidification and then over water in a final saturator, held at the flow reactor temperature, to attain 100 % humidity in this flow. The water reservoirs ($\sim$500 and $\sim$100 ml) and saturator ($\sim$10 ml; see the left side of Fig. 1) held deionized water and a few drops to a few ml of 96 % sulfuric acid to remove any amine or ammonia vapors that may come in with the carrier nitrogen or upon refilling with de-ionized water. A standard condition for nucleation experiments, called nucleation baseline conditions (NBC), had 27 % of the total flow directed over the water. The N_2 flow rate through the humidifier controlled the relative humidity of the system; this flow relative to the total flow yielded RH with NBC at 27 % RH. Dew point was routinely monitored and from it the calculated RH agreed with the RH from the relative flows to better than 2 % (Model 2000 Dewprime Dew Point Hygrometer, sampling about 2 % of the flow) for RH up to 45 %. At higher RH the humidified flow did not achieve saturation, e.g., at flows that should give 70 % RH, the hygrometer reading resulted in RH of 63–67 %.

Sulfuric acid was introduced by directing a portion of the carrier N_2 over a 303 K bulk solution of sulfuric acid, consisting of about 5 g of 96 % H_2SO_4 held in a glass saturator ($\sim$30 cm long: upper right in Fig. 1). A $\sim$15 cm length of 1/4″ OD teflon tubing carried this flow to the mixing region: its temperature generally stabilized at 29 ± 2 °C. It was not temperature regulated and at the beginning of each run its temperature rose steadily and stabilized after an hour or two. To change the amount of sulfuric acid, the carrier flow rate that was directed to the bulk sulfuric acid was changed. This differs from the approach employed by Ball et al., where the temperature of the bulk sulfuric acid was varied while the N_2 flow rate was held constant. Under NBC, the flow over bulk sulfuric acid was 1/6 the total flow, or about 1 sLpm. For other H_2SO_4 contents, this flow was varied from 0.4 to 2 sLpm. The concentration of sulfuric acid exiting the flow reactor was monitored with the Ambient Pressure Mass Spectrometer (AmPMS, Hanson et al., 2011) in negative ion mode (Hanson, 2005).

Near the bottom of the reactor, about 20 % of the total flow was sampled through a gently curved 30 cm length of 1/8″ OD stainless steel, then through $\sim$50 cm of 1/4″ OD copper tubing to an ultrafine condensation particle counter, UCPC (Stolzenberg and McMurry, 1991). The UCPC yields particle count rate data N_r (particle s^{-1}) and size (using pulse height analysis) information. A multichannel analyzer (EGG optics) recorded particle counts in a set time and this was divided by the live time (derived in Maestro software, EGG) to yield N_r: usually live time was 99 % or greater of real time except when nitrogenous bases were added. Pulse height information was recorded also however interpretation of this data is not straightforward as there are dependencies on particle composition that are difficult to quantify (Saros et al., 1996; Hanson et al., 2002; O'Dowd et al., 2004). The flow withdrawn by the UCPC was comprised of $\sim$1 sLpm transport flow and typically $\sim$0.3 sLpm condenser flow; the aerosol flow portion of the latter (i.e., capillary flow) was about 30 STP cm^3 min^{-1}. The condenser temperature was 8 °C and the saturator temperature was typically 40 °C with 1-butanol as the working fluid. Ball et al. (1999) employed the conditions outlined by Stolzenberg and McMurry (1991): 10 °C and 37 °C for condenser and saturator, respectively. Recently, Kuang et al. (2011) showed that the detection efficiency of this type of UCPC (butanol with a TSI 3025 or a modified 3020 TSI, Stolzenburg et al., 2011) can be greatly increased for particles in the 1.3 to 2.5 nm range by increasing the saturator temperature to 44 °C and the condenser flow rate to 0.47 sLpm. The UCPC was run in this enhanced mode for a variety of conditions to investigate particle detection efficiency: the resulting N_r scaled with aerosol flow which indicates measured particle number concentration N_p was unaffected. This indicates that the particle diameter was 2 nm or larger.

Number density (N_p, cm^{-3}) of particles was obtained by dividing N_r by the capillary flow rate, 0.5 or 0.7 cm^3 s^{-1}. Nucleation rate J was obtained by dividing N_p by an estimated nucleation time of 8 s, which has a high uncertainty of +100 %, −50 % (see the Supplement).

At the end of the flow reactor, a bell-shaped converging glass joint funneled the majority of the flow into the AmPMS, configured either with negative ions to detect sulfuric acid (Hanson, 2005, primary reagent ion $NO_3^- \cdot HNO_3$) or with positive ions to detect ammonia and amines ($H_3O^+ \cdot H_2O_n$ reagent ions, Hanson et al., 2003, 2011)(see Supplement). About 3/4 of the total flow was directed to AmPMS. The switch between negative ions and positive ions was readily executed by reversing the polarities of the voltages. The ion source flow was humidified with a $\sim$10 wt % HNO_3 aqueous solution which yields ppm levels of HNO_3 vapor in addition to H_2O vapor. With an ion drift length of 1.7 cm, a typical voltage drop of 0.84 kV, a typical bisulfate/nitrate ratio of $\sim$0.003 yields a sulfuric acid concentration of about 1.1×10^9 cm^{-3} for NBC (Hanson, 2011, with $kt = 2.6 \times 10^{-12}$ cm^3). Note that this detected value is an average of the H_2SO_4 concentration across the ion drift region which is affected by wall losses: along the flow reactor, the funnel, and the AmPMS sampling port and drift region. For example, the detection of sulfuric acid in Ball et al. was estimated to be only about 2-to-14 % of that present where particles were formed. Although the sampling arrangement is significantly different here, fluid dynamics simulations suggest that the current setup has a detection ratio of about 15($\pm$5) %, i.e.,

detected [H_2SO_4]/peak nucleation rate [H_2SO_4] (see Supplement, Panta et al., 2012).

To examine their effects on particle nucleation, ammonia or methyl amine was introduced to the system in a port just above the 296 K region ("top port"). The sources of these species were home-built permeation tubes operated at room temperature. The Teflon permeation tubes contained a small amount of liquid sample, ∼40 wt % methyl amine in water or ∼60 wt % ammonia in water (Sigma Aldrich), the tube ends were sealed by heating and inserting short lengths of glass rods. N_2 (∼100 STP cm^3 min^{-1}) was flowed over the tube, carrying the ammonia/amine that permeated the Teflon tubing to a two stage dynamic dilution system (right side of Fig. 1) before it entered the flow reactor. The permeation tubes were calibrated by titration with aqueous HCl by bubbling slowly (N_2 flow of ∼20 STP cm^3 min^{-1}) through dilute HCl solutions (Carlson et al., 2012). The permeation rates were relatively large (in pmol s^{-1}: 50 for NH_3 and 80 for CH_3NH_2) necessitating the use of a serial dynamic dilution system so that concentrations of ∼1 ppmv base in the N_2 flow over the perm tubes were reduced by factors of $\sim 10^5$ if fully mixed with no losses into the 6 sLpm flow.

A base mixing ratio of a few tens of pptv in the flow reactor could be reliably prepared which was checked with AmPMS by adding the bases to the flow through a port at the bottom of the flow reactor. AmPMS detection of ammonia or amine when it was added at the top port was much less than the amount added. Note that the background levels for the ions of interest (NH_4^+ and $CH_3NH_3^+$) (Hanson et al., 2011) are substantial: for these experiments, count rates at these masses give mixing ratios of approximately 100 pptv and 3 pptv respectively.

The zeroing mechanism for AmPMS led to severe loss of [H_2SO_4] and thus was not used for the experiments described here. After these experiments were performed, AmPMS was attached to the flow reactor with the zeroing mechanism to better quantify N-base. No ammonia or amines were detected (see Supplement for a plot of the amines). Upper limits to the methyl and dimethyl amine mixing ratios in the effluent of the flow reactor were 0.3 and 1 pptv, respectively. Ammonia had a poor detection limit for this measurement due to a high background, 4 ppbv equivalent, and an upper limit of 170 pptv was determined. The high background for ammonia was due to a previous exposure to outdoor air when AmPMS sampled ambient air for several weeks.

A custom-built differential mobility analyzer (geometrically equivalent to a TSI long model 3071) was used to size the particles for two sets of sulfuric acid flow rates at 68 % RH. Due to a previous exposure, trace nitrogen bases were present in the high H_2SO_4 run while ∼30 pptv NH_3 was added for the low H_2SO_4 run. These bases resulted in particle numbers much higher than neat H_2SO_4-H_2O which allowed for a size distribution measurement; neither base was detected with AmPMS (less than 0.5 pptv). A homemade ∼10 µCi particle charger was used and the charging efficiency of Fuchs (1963) was applied along with particle loss within the analyzer (Birmili et al., 1997).

Shown in Table 1 are the typical operating conditions and experimental parameters for the nucleation data presented here. Standard RH and sulfuric acid conditions were chosen (NBC) so that reproducibility and stability of the system over long periods of time could be monitored. The sulfuric acid laden flow was 1 sLpm, the humidified flow was 1.6 sLpm, and the remainder of 3.4 sLpm was dry N_2 that entered the mixing region along with the humidified flow. To achieve a range of H_2SO_4 content and RH, flows were varied over the range of 0.4-to-2 sLpm, 0.8 to 4 sLpm, and 1 to 4 sLpm, respectively, always maintaining a total of 6 sLpm. Temperatures of the mixing region (313 K), the nucleation region (296 K) and the bulk sulfuric acid (303 K) were held constant except for some diagnostic experiments when the temperature of the mixing region was varied to demonstrate suppression of nucleation that can occur during mixing of the reagents. The properties of the nucleation region were taken to be those of Ball et al. who determined experimentally that maximum nucleation rates occurred about 20 cm into the cooled nucleation region at a temperature about 2 K warmer than the walls. Therefore the nucleation rates reported here are for a temperature of 298 (±2) K. Note that RH values are reported for 296 K: the RH in the region for maximum nucleation are about 0.9 times the values quoted here. Discussed in the Supplement are the significant differences in the experiment from that published in Ball et al. (1999).

3 Results

To check for stability of the system, at the beginning of each measurement sequence and often at the end of a run, the flow of gases was set to standard conditions, NBC. Table 1 shows a summary of NBC for the entire system. Several runs with NBC as well as 27 % RH data at different Q_A (the nitrogen flow rate through the sulfuric acid reservoir) are compiled in Fig. 2 which plots measured N_r vs. Q_A. The mass spectrometer was not operational for many of the measurements in this figure, but when concurrently running, measured [H_2SO_4] was linearly proportional to Q_A up to ∼1.5 sLpm (see Supplement). Above 1.5 sLpm, [H_2SO_4] does not increase in a linear fashion with Q_A, due to finite rates of diffusion, etc. In Fig. 2, the particle count rate at $Q_A = 2$ sLpm falling below the typical power dependency line is due to operation in this region of Q_A. The scatter in the results widens as [H_2SO_4] decreases. The number of background particles (i.e., generated via moving parts in the gas regulator or valves or due to small leaks in the UCPC sampling line) was generally low, typically 2–10 particles counted in 100 s, but at times was as high as 0.5 s^{-1}. The background particle count rate was determined about once per run by switching to $Q_A = 0$. Upon returning to NBC, N_r might take an hour to return to normal

Table 1. Nucleation Baseline Condition temperatures and flows and experimental temperatures, range of flows, and other conditions.

Parameter	Temp (K)	Flow (sLpm)	Range (sLpm)	RH, P, or $[H_2SO_4]$
Dry Nitrogen	–	3.4	1–4.5	
Humid Nitrogen	296	1.6	1.2–4	15-to-68 % RH
Q_A, H_2SO_4 Flow	303	1.0	0.4–2	0.2-to-2 $\times 10^{10}$ cm^{-3} [a]
Mixing Region	313	6	4–7	0.97 atm
Flow Reactor	296[b]	6		~1 in. H_2O gauge[c]
NBC Dew Point	276	–	–	27 % RH[b]

[a] This is the range of $[H_2SO_4]$ (total: monomer + hydrates) estimated where nucleation rate peaks.
[b] 298 K where maximum nucleation occurs; RH in this region will be 0.9 times the RH values that are reported for 296 K.
[c] Ambient pressure was typically 0.95-to-0.99 atm; pressure difference between flow reactor and ambient was ~0.003 atm.

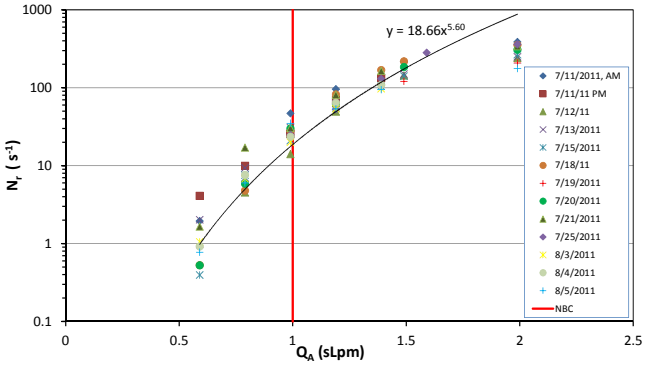

Fig. 2. Particle count rates plotted versus flow through the sulfuric acid reservoir, RH at 27 %, $T = 296$ K. NBC is $Q_A = 1$ sLpm and N_r shows a variability of a factor of ~2 (×2, ÷2) over weeks. A typical power dependency is shown for these conditions.

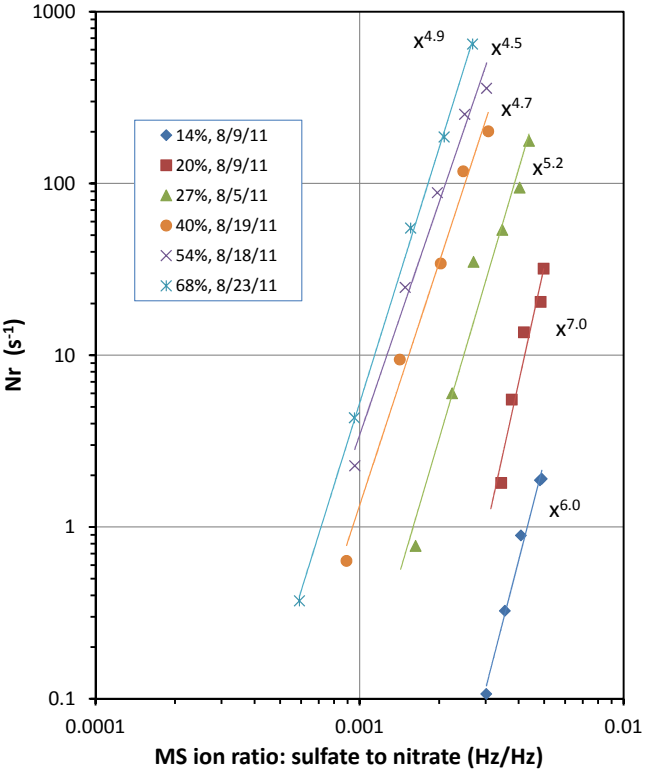

Fig. 3. Particle count rates N_r vs. ion ratio (HSO_4^- core ion count rate/NO_3^- core ion rate) observed with the mass spectrometer. The average H_2SO_4 concentration across the ion-molecule drift region, about 1.7 cm long, is given approximately by the ion ratio times 3.8×10^{11} cm^{-3} while the nucleation zone peak H_2SO_4 is 5-to-10 times this. A range of RH conditions are shown here with power dependencies of 5–7.

levels, so that more frequent monitoring of the background particles was impractical.

The clustering of data shows the consistency of reactant and flow conditions over an extended period of time. The power dependency on H_2SO_4 remained relatively constant over that time period, averaging roughly 5.5. For these conditions with the assumption that $[H_2SO_4]$ is proportional to Q_A when it is below 1.5 sLpm, the critical cluster has ~5.5 sulfuric acid molecules. Finally, the reproducibility of NBC data was used as a monitor of the system: if particle count rates were outside the range of 20 ± 10 Hz at NBC, there was some change in the system, e.g., a temperature control issue, a potential contaminant, water reservoirs need filling, leak, flow meter malfunction, UCPC needs service etc. A plot of particle count rates for NBC over a ~10 month period is displayed in the Supplement.

Shown in Fig. 3 is the particle count rate data at several RH vs. AmPMS ion ratio which is linearly proportional to $[H_2SO_4]$ at a given RH. These data show power dependencies of 4.5 to 6, with perhaps slightly lower values on average at the higher RH, however not appreciably greater than the scatter. The variation of the power dependency on H_2SO_4 with RH seems to be muted over this range of RH, 14–68 %. A larger set of data is presented in the Supplement.

There is a strong dependency on RH of N_r and thus the nucleation rate. As demonstrated in Fig. 3 when RH increases so does the number of particles detected by the UCPC. At 14 % RH, there are very few particles at 0.0026 ion ratio (equivalent to $\sim 1 \times 10^9$ cm^{-3}) given by the nominal flow rate

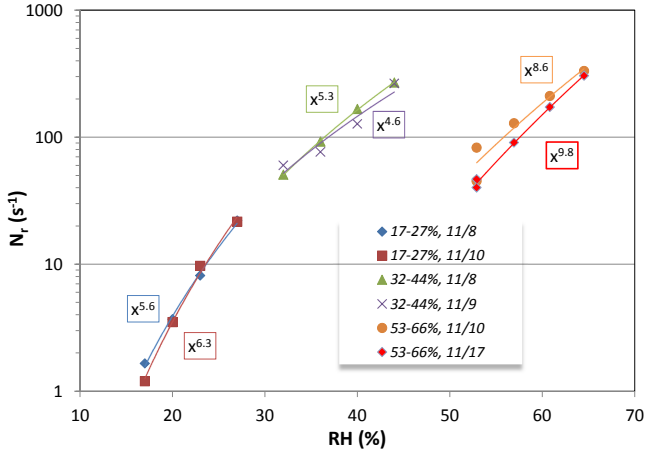

Fig. 4. Variation of N_r with RH at constant [H_2SO_4] (plus hydrates). $Q_A = 1$ sLpm for the low RH (17–27 %) and medium RH (32–44 %) variations and 0.5 sLpm for the high RH variation (53–66 %). The power dependencies are shown in the figure.

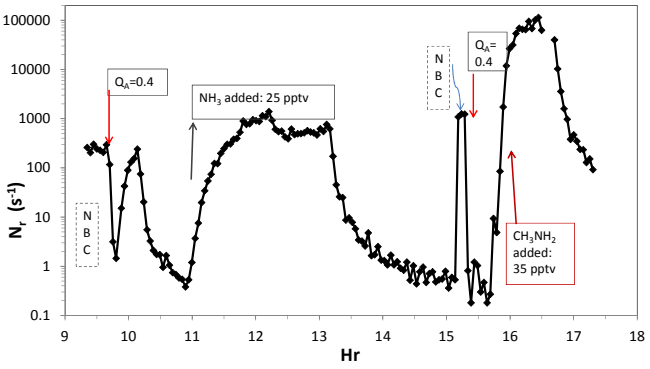

Fig. 5. N_r plotted versus time for N base additions to the top port. N_r is greatly affected for $Q_A = 0.4$ sLpm, 27 % RH conditions where $0.05\,s^{-1}$ is typical for pristine conditions. NBC was checked twice during the experiment (09:30 and 15:15) and undetectable, residual N base exhibited a significant effect. AmPMS showed a detectable amount of methyl amine during its addition.

over the bulk sulfuric acid (1.0 sLpm). At 20 % RH for the same ion ratio, there is about a factor of 20 increase in N_r and at 27 % RH there is an additional factor of ten increase. Further increases in RH at the same ion ratio give a larger number of particles, e.g., at 68 % RH, there was another factor of 50 increase in the particle count rate detected at the same sulfuric acid ion ratio.

Note that run-to-run variations in N_r of 50 % for NBC were not uncommon and are believed to be due to variations in room temperature that affect which portion of the flow is sampled by the UCPC: coupled with radial gradients in particle concentrations (Ball et al., 1999) temperature dependent scatter can be introduced. Also, there were small variations in the position of the inlet. Room temperature also affects the temperature of the tubing carrying the H_2SO_4 laden flow to the mixing region. Furthermore, when H_2SO_4 vapor was monitored with the mass spectrometer and particle count rates were plotted against this measurement, scatter day-to-day was at times larger than ±50 %. Variable temperatures could lead to variations in mixing and losses in the room temperature section and thus variations in mass spectrometer derived H_2SO_4 concentrations.

Variations of N_r with RH were investigated over small ranges in RH while maintaining a constant flow over the bulk sulfuric acid, Q_A. The results are plotted in Fig. 4 and they show power dependencies on RH of 6.1 over the range 17-to-27 % RH, 5.4 over the range 32-to-44 % RH, and 7.6 for 53-to-67 % RH. These were obtained by keeping Q_A constant while varying the RH with $Q_A = 1$ sLpm for the low and medium RH runs and 0.5 for the high RH experiment. The mass spectrometer was also sampling and measured H_2SO_4 was constant to within 5 % during each run.

3.1 Ammonia and amine addition

Ammonia and methyl amine were introduced separately but in the same manner so that their relative efficacy in generating particles could be assessed. These experiments were conducted at 27 % RH and at a Q_A of 0.4 sLpm, which yields particle count rates of $0.05\,s^{-1}$ or lower (i.e., background) in the absence of added species. Either methyl amine or ammonia were introduced to the system just below the mixing region (top port) at a rate that would give calculated mixing ratios of 2-to-50 pptv if fully mixed and absent wall losses during mixing. N-base mixing ratios quoted here are those estimated from the measured permeation rates and the known dilutions. Note that a 3-D computational fluid dynamics simulation of a similar experiment has been performed (Hanson and Eisele, 2002) and NH_3 was shown to diffuse rapidly when added in this manner. An experiment is depicted in Fig. 5 where particle count rates are plotted as a function of time.

Initially, N_r for NBC was a factor of ten greater than normal, due to a previous exposure of tubing to amines. At ∼09:50 LT, NBC was adjusted to very low Q_A, 0.4 sLpm, and NH_3 was turned on and after ∼30 min it was shut off and N_r was seen to rapidly decrease below $1\,s^{-1}$ which is above the $\sim 0.05\,s^{-1}$ rate for the neat 27 % RH system: this previous exposure to ammonia, and possibly the previous day's amine experiment, had not time to flush out.

NH_3 was fully introduced at around 11:00 and particle numbers increased substantially; an adjustment to the dilution system to maintain 25 pptv is evident at 12:15. After a few hours, N_r was equal to $\sim 500\,s^{-1}$. This is an enhancement of about a factor of 10^4 over the neat system for these conditions. At about 13:10 the ammonia perm tube flow was diverted from the dilution system, keeping the last two stages of flow going through the dilution system and into the

reactor, and the particle numbers can be seen to decrease at first rapidly and then gradually over the next few hours. At 15:15, conditions were set to NBC and N_r was about 50 times normal NBC, even larger than the 09:30 value; this was due to low (sub-pptv?) levels of ammonia introduced into the system with the last two stages of the dilution system.This residual ammonia or "contaminant" coming from the tubing in the dilution system was confirmed in separate experiments by shutting off all the dilution flows whereupon NBC gave normal N_r ($\sim$20 s^{-1}) almost immediately. Q_A was reset to 0.4 sLpm at 15:30.

At 15:50 methyl amine was added at about a 35 pptv level. Particle numbers increased rapidly and continued to grow such that the live time percentage of the instrument decreased below 0.05 %. Because the live time correction for this data is not reliable and because butanol vapor depletion within the UCPC can be significant (Saros et al., 1995) at high numbers, the 10^5 s^{-1} rate indicated in the figure is a lower limit. The enhancement factor for 35 pptv methyl amine is of the order of 10^6 or higher.

AmPMS monitoring of methyl amine during this time period showed an increase of about 0.4 pptv above ion background signal (30 Hz signal equivalent to 3.2 pptv). Methyl amine is exposed to surfaces between the top port and the mass spectrometer and a large loss is not surprising (about a factor of 100, i.e., 1 % of the added methyl amine reached AmPMS) because surfaces have been exposed to sulfuric acid vapor and particles for thousands of hours. Note that ammonia addition did not lead to a detectable increase in AmPMS signal on a background ion count rate of about 1 kHz (equivalent to $\sim$90 pptv.)

A second set of experiments for similar conditions were performed where ammonia was introduced at $\sim$20 pptv and N_r was 1000 s^{-1}, which agrees with the result above, within uncertainties. Then methyl amine was swapped in and its level was adjusted so that particle count rates matched that for 20 pptv ammonia: that was a level of about 3 pptv methyl amine. Note that once exposed to methyl amine, the dilution system required tens of hours to recover. The longer the exposure to amine, the longer the time needed to cleanse the dilution tubing system, which points to a possible mechanism: the longer the Teflon tubing is exposed to amine, the more is able to diffuse into it, to be later entrained into clean gas. A few days after this experiment, a final experiment with ammonia addition at levels of 2 and 45 pptv resulted in N_r of 40 and 7000 s^{-1}, respectively.

Although much lower than the added ammonia, it is possible that there was enough residual methyl amine introduced to affect particle formation rates. Likewise, there was probably residual ammonia when methyl amine was sent through the dilution system. In the latter case, however, the residual ammonia probably did not significantly affect the N_r during methyl amine addition, due to methyl amine's much larger effect.

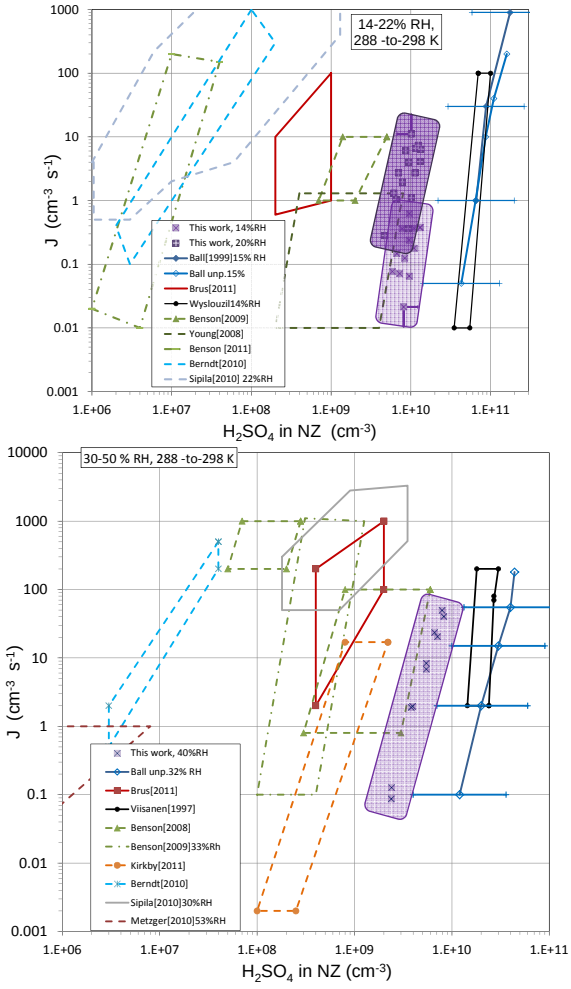

Fig. 6. Comparison of results from this work (purple + and X) to previous work at relative humidities of **(a)** $\sim$16 % and **(b)** $\sim$40 % where nucleation rate J is plotted against H_2SO_4 concentration. Those studies with solid lines are results using H_2SO_4 vapor from sulfuric acid solutions entrained in a flow of gas (bulk) while those with dashed lines use photo-oxidation of SO_2 as a source of H_2SO_4. The reported temperatures for the studies are 298 K except 288 K for Benson et al. (2008, 2009, 2011) and Young et al. (2008); 292 K for Kirkby et al. (2011). Typical error bars due to uncertainties in nucleation zone concentration and residence time are shown for two points in **(a)**. Note that $[H_2SO_4]$ for the Ball et al. (1999) unpublished work shown here was measured with an ion-drift arrangement similar to that used here and a factor of 10 (+200/−66 %) was applied to get $[H_2SO_4]_{NZ}$.

3.2 Particle size

The size distributions of particles generated in the nucleation flow reactor measured with the differential mobility analyzer indicate peaks of $\sim$7.7 nm diameter for $Q_A = 1.0$ sLpm and $\sim$6 nm for $Q_A = 0.4$ sLpm. See the Supplement for size distributions. These sizes are in agreement with those reported by Ball et al. and are well above the lower limit of

Table 2. Comparison of H_2SO_4 Power Dependencies at various RH.

RH	This work[a]	Ball et al. (1999)[b]	Wyslouzil et al. (1991)[a]	Viisanen et al. (1997)[a]	Young et al. (2008)[c]	Benson et al. (2006, 2008 2011)[c]	Berndt et al. (2005, 2006 2010)[d]	Brus et al. (2010 2011)[e]	Kirkby et al. (2011)[f]
14–16	5.5 ± 1.5	7–8	16		4–8	2.3, 4.5	5	1.5	
20–23	5 ± 2	–			3	5.3	4, 2	–	
25–33	6 ± 1	7	16		–	5.6–10	3	6, 1.3	
35–44	5 ± 0.5			20	–	6.3		–	6
45–55	4 ± 0.5			10			3, 1.9	8	
57–70	4.2 ± 0.6						1.9	1.7	

[a] $T = 298$ K, [b] 297 K; data at 32 % RH was not published, [c] 288 K, [d] 293 K, [e] 299 K ?, [f] 292 K

detection for the UCPC. This is supported by the observation that changing the UCPC conditions to those of Kuang et al. (2012) made no significant difference in N_p. See the Supplement for more discussion of UCPC conditions. At $[H_2SO_4]$ levels of 10^{10} cm^{-3}, the rough diameter growth rate is $\sim$0.4 nm s^{-1} which along with a 10–20 s exposure time results in particle diameter increases of 4 to 8 nm.

4 Discussion

4.1 Power dependency on H_2SO_4

The power dependency (PD_1) of the observed number of particles on sulfuric acid concentration have been reported in a number of studies and are compared in Table 2 where the H_2SO_4 power dependencies along with experimental conditions are listed. Previous work for experiments of 14 % RH and higher are included and results for many studies have power dependencies of 5 or above. A few recent studies report very low values of $\sim$1.5: the authors (Berndt et al., 2010; Sipilä et al., 2010) speculate that their particle detection efficiency was much better than all earlier work, implying a deficiency in earlier work that hid the low power dependency. However, the most recent Kirkby et al. (2011) study using identical particle instrumentation obtained $\sim$6 for PD_1, seeming to settle the debate. Furthermore, the sizes of the particles detected in this study were shown to be well above the detection threshold for the UCPC as deployed.

The power dependency reported here of 4-to-7 near 15 % RH is less than the 7-to-8 of Ball et al. (1999); however the small range of H_2SO_4 explored in the present work and low particle count rates limits the significance of that comparison. Previous work by Young et al. (2008) at 15 % RH show a PD_1 of $\sim 6 \pm 2$, which is also consistent with the present and Ball et al. results. Other work by this group at 9–16 % RH (Benson et al., 2008, 2011) report lower values of 2–5 for PD_1. At 27 % RH, however, these authors are in better agreement with the present PD_1 of 6 ± 2: Benson et al. (2008, 2009) report for RH of 22-to-30 % PD_1 of 5.6-to-9.5. For the range 35–44 % RH, PD_1 of the present work 5 ± 1 agrees well with Kirkby et al. (2011) and the earlier work of Brus et al. (2010) but not the PD_1 of Brus et al. (2011). Explanations for these discrepancies are based on experimental conditions or techniques, such as deficient particle counters or contaminant species.

The power dependencies on H_2SO_4 reported here vary modestly with RH as it increases above 14 %. The general trend is consistent with the Ball et al. study who found lower PD_1 at higher RH. The present results indicate that for $[H_2SO_4]$ of $\sim$3–10 $\times$ 10^9 cm^{-3}, n_1 varies from $\sim$5.5 at 20 and 27 % RH, to 5.0 for 40 % RH and about 4 for 54 and 68 %. It appears that for the $[H_2SO_4]$ explored in this study, at high RH the number of H_2SO_4 molecules in the critical cluster n_1 is as small as 4. This is significantly smaller than the power dependencies in the 8-to-12 range found at lower humidity (Ball et al., 1999, 2-to-10 % RH): a higher PD_1 at lower RH is expected according to theory (Vehkamäki et al., 2002).

4.2 Comparison of J and $[H_2SO_4]_{NZ}$

Comparisons of nucleation rates J as a function of $[H_2SO_4]_{NZ}$, the H_2SO_4 concentration in the nucleation zone, i.e., where particles are formed, depend on knowledge of nucleation times and sulfuric acid losses. Generally, nucleation studies have limited accuracy for the estimates of these quantities, including the present study. Detailed knowledge of flows, temperatures, exposure times and wall losses obtained from computational fluid dynamics can be helpful (e.g., Hermann et al., 2010). The flow reactor and nucleation have been simulated using computational fluid dynamics (Panta et al., 2012). Preliminary results show (see Supplement) a factor of 7 difference between $[H_2SO_4]_{NZ}$ and the measured $[H_2SO_4]$.

These estimates were applied to the particle number densities N_p and measured $[H_2SO_4]$ to give J and $[H_2SO_4]_{NZ}$. The +100/−50 % uncertainty in the nucleation time dominates the additional systematic error in J and the +40/−30 % uncertainty in the factor of 7 dominates that for $[H_2SO_4]_{NZ}$. The J values are plotted vs. $[H_2SO_4]_{NZ}$ in Fig. 6 for the (a) 14 % RH results and (b) for the 40 % RH results along with a number of previous studies. Each set of results is depicted

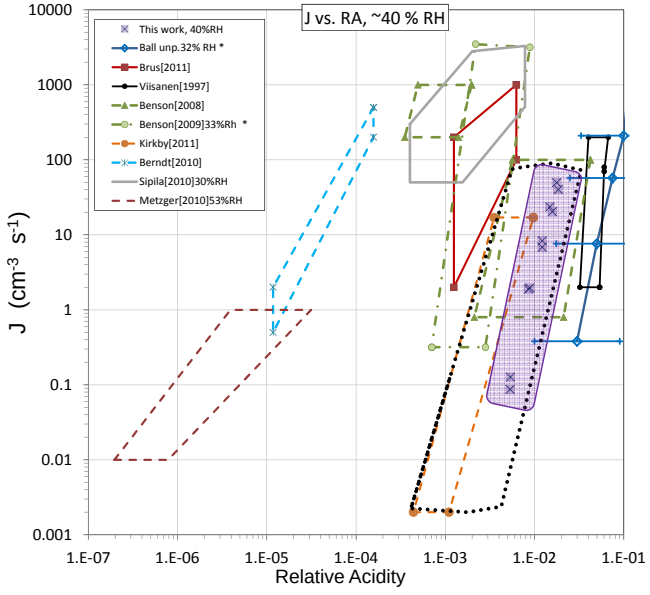

Fig. 7. As in Fig. 6 but nucleation rate J is plotted against RA for 40 % RH. For two studies (denoted with *) with results at 32 and 33 % RH where RH dependence was quoted, J was corrected to 40 % RH equivalent using PD_2 = 6. For three other studies conducted at RH significantly different from 40 %: the Sipila et al. (2010) results for 30 % RH if corrected in a similar manner would cause further divergence while results for Metzger et al. (2010) (53 %) and Berndt et al. (2010) (45 %) would diverge less (J lowered by a factor of 4 and 2 respectively).

as an area on the plot that encompasses the reported uncertainties in J and H_2SO_4 concentration. A few of the studies were performed at lower temperatures, which could explain some of the differences with the present results (e.g. see Fig. 7 below), but the overall wide range in nucleation rate results is not entirely due to temperature differences. Taken as a whole, it appears that using a photolytic source to oxidize SO_2 could lead to nucleating species more efficient than bulk H_2SO_4. However, scatter in the data and the latest photolysis experiment at 38 % RH (Kirkby et al., 2011) who report significant amounts of amines in the particles, suggest that measured Js are easily skewed high possibly due to nitrogenous bases that could not be detected in the gas phase. This explanation is bolstered by our observation that a million-fold increase in N_r can be achieved with addition of methyl amine at ~30 pptv but because of loss was detected at only a 0.4 pptv level. A few studies have suggested that contaminants may have been present (Benson et al., 2011; Kirkby et al., 2011; Brus et al., 2011).

This observation along with the variety of results displayed in Fig. 6, suggests that undetected base contaminant at the pptv level could be a common problem, significantly affecting particle formation rates. For the present experiment, the level of amine needed to significantly affect the results can be estimated. Applying an extrapolation of the N_r in Table 4 using a power dependency on a base of 1.5 (see below), about 10 ppqv (10 fmol mol^{-1}) of methyl amine could give a particle formation rate equal to the 0.05 s^{-1} rate that is believed due to the neat H_2SO_4-H_2O system. A level of 10 ppqv is undetectable with the current instrumentation and a potential effect due to this level of base cannot be ruled out. Please see the Supplement for further discussion of this point.

4.3 Water content of critical cluster

The variation of N_r with RH yields experimental power dependencies $PD_{2,exp}$ of J on RH of 5 to 8; if taken at face value, these $PD_{2,exp}$ indicate that there are 5–8 water molecules in the critical cluster. Yet the measurements do not adhere to the constrictions imposed by the nucleation theorem for binary systems (Oxtoby and Kashchiev, 1994) where the activity of the second component must be held constant while the other component's activity is varied. Here, while total H_2SO_4 was held constant as RH was varied over a small range, the H_2SO_4 activity was not constant due to changing hydration of H_2SO_4 molecules. Whether the bare monomer activity is the relevant parameter for nucleation calculations using the classical liquid drop model was explored by Bein and Wexler (2007). Extending those ideas leads to the following treatments for the number of water molecules n_2 in the critical cluster: (i) the observed nucleation rates as a function of RH can be corrected for changes in monomer activity, i.e., normalized, and (ii) taking advantage of the quasi-equilibrium assumption and accounting for the hydration of the main nucleating species that is on average a well-hydrated H_2SO_4 molecule.

4.3.1 Normalized to H_2SO_4 activity

Using the equilibrium constants for adding water molecules to sulfuric acid (Mirabel and Ponche, 1991; Noppel, 2000; Hanson and Eisele, 2000) the relative amounts of monomer H_2SO_4 at each RH were calculated. Then the observed rates were normalized to constant monomer H_2SO_4 activity, a_1, using the observed H_2SO_4 power dependencies, n_1, of 5.5, 5, and 4 for the low, middle and high RH results.

$$J' = a_1^{-n_1} J \tag{1}$$

$$n_2 = \frac{\partial \ln J'}{\partial \ln \mathrm{RH}} = -n_1 \cdot \frac{\partial \ln a_1}{\partial \ln \mathrm{RH}} + \frac{\partial \ln J}{\partial \ln \mathrm{RH}} \tag{2}$$

where J' is the normalized rate and J is the measured rate. For small changes in RH, n_1 can be taken to be constant in Eq. (2). Assuming the nucleation time does not vary with RH, J can be replaced by particle count rates N_r. A set of normalized rates J' (then renormalized to the lowest activity J) are shown in Table 3 for the different ranges of RH results and their power dependencies on RH are ~12-to-15. This treatment indicates there are 12-to-15 H_2O molecules in the critical cluster for these conditions.

Table 3. H_2O Power Dependency Treatments due to H_2SO_4 hydration[a].

RH	Expt'l	Monomer fraction	Normalized N_r (s^{-1})	Eq. (1) with N_r, n_2[b,d]	Average hydrate no.	n_2 using Eq. (3)[c,d]
17–27	6	0.3–0.19	$1.3–3\times10^2$	12	1.05	11.8
32–44	5	0.15–0.095	$60–3\times10^3$	12.5	1.43	12.2
53–67	9.2	0.07–0.045	$60–4\times10^3$	15.5	1.81	16.4

[a] Equilibrium constants $K_{w,w-1}=[H_2SO_4\cdot(H_2O)_w]/[H_2SO_4\cdot(H_2O)_{w-1}]$RH with RH in %. $1/K_{w,w-1}=10$, 50, 166, 200, 300 % for the 1st through 5th hydrates.
[b] PD_2 of normalized N_r: method (i) in text.
[c] Expt'l PD added to hydrate no. times 5.5, 5 and 4, respectively: method (ii), Eq. (3), in text.
[d] Propagation of random errors leads to ±1-to-1.5 precision uncertainty in n_2.

4.3.2 H_2O with the H_2SO_4 hydrates

An alternative line of reasoning takes into account the number of water molecules on average that arrive with each H_2SO_4 molecule that are in the critical cluster. It is assumed that the $PD_{2,exp}$ on RH of the observed rate J is the extra waters beyond the average number carried in with each monomer. Then the number of waters in the critical cluster, n_2 is given by

$$n_2 = PD_{2,exp} + n_1 \cdot \text{(average hydration number of } H_2SO_4) \quad (3)$$

With the equilibrium constants for monomer hydration (equilibrium constants in 1/% RH are given in Table 3), the average number of hydrate water molecules on an H_2SO_4 are 1.05 ± 0.14, 1.43 ± 0.11, and 1.81 ± 0.11 for the low, middle and upper RH ranges, respectively. Multiplying these by the H_2SO_4 power dependencies n_1 and adding to the H_2O power dependency for total H_2SO_4 constant (the experimental column), yields the values in the last column. The result is that about 12–16 water molecules are present in the critical cluster. The agreement between these two methods is not purely coincidental as they are essentially the same mathematically: the average hydration number is closely related to the variation of a_1 with RH.

4.4 *J* versus Relative Acidity for 40 % RH

To take into account temperature differences, the data shown in Fig. 6b is plotted vs. relative acidity (RA, the partial pressure of H_2SO_4 divided by the saturation partial pressure Ayers et al. (1980)) in Fig. 7. When plotted in this way, there is better agreement amongst the published data with a few exceptions: Metzger et al. (2010), Berndt et al. (2010), Sipila et al. (2010), and the Fig. 1a data of Benson et al. (2008) (the Fig. 1b data of this reference agrees well.) Note that an $PD_{2,exp}$ = 6 was applied to the 33 % RH Benson et al. (2009) data and to the 32 % RH unpublished Ball et al. data. Most of the data in Fig. 7 cluster around the present data and that of Kirkby et al. (2011).

Table 4. Ammonia and amine addition experiments at 27 % RH.

N base	Level, pptv	N_r (s^{-1})	J ($cm^{-3}\,s^{-1}$)[a]	EF
–	0	<0.05	<0.01	–
CH_3NH_2	3	1000	125	2×10^4
CH_3NH_2	35	$>10^5$	$>10^4$	$>2\times10^6$
NH_3	2	40	5	800
NH_3	20	1000	125	2×10^4
NH_3	45	7000	875	1.4×10^5

[a] $J=N_r$ divided by aerosol sampling rate of 0.7 $cm^3\,s^{-1}$ divided by ~8 s nucleation time. [b] Enhancement factor over neat H_2SO_4-H_2O system for $Q_A=0.4$ sLpm where $[H_2SO_4]$ at the peak of nucleation is $\sim3\times10^9$ cm^{-3}.

A relative acidity of 4-to-8×10^{-3} gives a nucleation rate of 1 $cm^{-3}\,s^{-1}$ at 40 % RH. Assuming the J vs. RA relationship does not vary with temperature, this RA is achieved at 252 K for an atmospheric $[H_2SO_4]=10^7$ cm^{-3}. These temperatures are not present for most boundary layer nucleation studies (McMurry et al. (2000)), and the present measurements indicate that binary nucleation is not a likely contributor to new particle formation events in this region of the atmosphere. As suggested by Weber et al. (1999), however, $[H_2SO_4]$ and temperatures near the outflow of clouds can lead to RA up to 0.01, indicating that binary nucleation can play a role in nucleation in the middle to lower troposphere.

5 Ammonia and amines

Table 4 contains the particle count rates for the ammonia and methyl amine addition experiments. These were taken for the following experimental conditions: 27 % RH and $[H_2SO_4]$ in the nucleation zone of $\sim3\times10^9$ cm^{-3} where in the absence of base, particle count rates are 0.05 s^{-1} or less. Methyl amine is roughly 25 to 100 times more effective than ammonia when added at similar levels. This experiment result is in agreement with earlier work (Kurten et al., 2008; Berndt et al., 2010; Erupe et al., 2011) that amines are effective in promoting nucleation involving sulfuric acid.

The data in Table 4 are consistent with power dependencies of particle count rates on methyl amine of about 2 and

on ammonia of about 1.5. More experiments are planned investigating the effects of bases on nucleation including dependencies on [base], [H_2SO_4], and RH. Also, the amounts of residual amines in the dilution system and their affect on particle formation rates will be explored.

Atmospheric levels of methyl amine are <1 % of ammonia throughout much of the atmosphere (Ge et al., 2011; Hanson et al., 2011) and the data in the table suggests that ammonia need only be about 30 pptv to have the same effect as a typical atmospheric level of 3 pptv for methyl amine. These addition experiments were carried out with $[H_2SO_4]_{NZ}$ estimated to be about 3×10^9 cm^{-3}. This is much higher than is found in the atmosphere: daytime atmospheric levels are only about 1/100 of this value (McMurry et al., 2000). Although more experimental data are required before these measurements can be applied to atmospheric conditions, the data suggests that with ammonia levels about 1000 times methyl amine levels (Nowak et al., 2005; Hanson et al., 2011), ammonia may play a larger role than does methyl amine. Yet there are a large number of amines in the atmosphere of greater abundance than methyl amine (Ge et al., 2011; Hanson et al., 2011); more data on the effects of these amines on nucleation are needed.

Supplementary material related to this article is available online at: http://www.atmos-chem-phys.net/12/4399/2012/acp-12-4399-2012-supplement.pdf.

Acknowledgements. This work was supported by NSF Grants 0943721, 1068201, and 1051396. Augsburg College's URGO program is acknowledged for funding travel and summer support. Correspondence with S. Clegg, A. Wexler, and E. Bien on H_2SO_4 activity and S. Clegg regarding methyl amine in E-AIM model is gratefully acknowledged.

Edited by: K. Lehtinen

References

Ayers, G. P., Gillet, R. W., and Gras, J. L.: On the vapor pressure of sulfuric acid, Geophys. Res. Lett., 7, 433–436, 1980.

Ball, S. M., Hanson, D. R., Eisele, F. L., and McMurry, P. H.: Laboratory studies of particle nucleation: Initial results for H_2SO_4, H_2O, and NH_3 vapors, J. Geophys. Res., 104, 23709–23718, 1999.

Bein, K. J. and Wexler, A. S.: Interpreting activity in H_2O-H_2SO_4 binary nucleation, J. Chem. Phys., 127, 124316, doi:10.1063/1.2768925, 2007.

Benson, D. R., Erupe, M. E., and Lee, S. H.: Laboratory-measured H_2SO_4-H_2O-NH_3 ternary homogeneous nucleation rates: Initial observations, Geophys. Res. Lett., 36, L15818, doi:10.1029/2009gl038728, 2009.

Benson, D. R., Young, L. H., Kameel, F. R., and Lee, S.-H.: Laboratory-measured nucleation rates of sulfuric acid and water binary homogeneous nucleation from the SO_2 + OH reaction, Geophys. Res. Lett., 35, L11801, doi:10.1029/2008GL033387, 2008.

Benson, D. R., Yu, J. H., Markovich, A., and Lee, S.-H.: Ternary homogeneous nucleation of H_2SO_4, NH_3, and H_2O under conditions relevant to the lower troposphere, Atmos. Chem. Phys., 11, 4755–4766, doi:10.5194/acp-11-4755-2011, 2011.

Berndt, T., Böge, O., Stratmann, F., Heintzenberg, J., and Kulmala, M.: Rapid formation of sulfuric acid particles at near-atmospheric conditions, Science, 307, 698–700, 2005.

Berndt, T., Boge, O., and Stratmann, F.: Formation of atmospheric H_2SO_4/H_2O particles in the absence of organics: A laboratory study, Geophys. Res. Lett., 33, L15817, doi:10.1029/2006GL026660, 2006.

Berndt, T., Stratmann, F., Sipilä, M., Vanhanen, J., Petäjä, T., Mikkilä, J., Grüner, A., Spindler, G., Lee Mauldin III, R., Curtius, J., Kulmala, M., and Heintzenberg, J.: Laboratory study on new particle formation from the reaction OH + SO_2: influence of experimental conditions, H_2O vapour, NH_3 and the amine tert-butylamine on the overall process, Atmos. Chem. Phys., 10, 7101–7116, doi:10.5194/acp-10-7101-2010, 2010.

Birmili, W., Stratmann, F., Wiedensohler, A., Covert, D., Russell, L. M., and Berg, O.: Determination of Differential Mobility Analyzer Transfer Functions Using Identical Instruments in Series, Aerosol Sci. Technol., 27, 215–223, 1997.

Brus, D., Hyvärinen, A.-P., Viisanen, Y., Kulmala, M., and Lihavainen, H.: Homogeneous nucleation of sulfuric acid and water mixture: experimental setup and first results, Atmos. Chem. Phys., 10, 2631–2641, doi:10.5194/acp-10-2631-2010, 2010.

Brus, D., Neitola, K., Hyvärinen, A.-P., Petäjä, T., Vanhanen, J., Sipilä, M., Paasonen, P., Kulmala, M., and Lihavainen, H.: Homogenous nucleation of sulfuric acid and water at close to atmospherically relevant conditions, Atmos. Chem. Phys., 11, 5277–5287, doi:10.5194/acp-11-5277-2011, 2011.

Carlson, K. K., Panta, B., Glasoe, W. A., and Hanson, D. R.: Ammonia and Amine Permeation Tubes: Quantification, Use in AmPMS Calibrations and in Nucleation Experiments, in preparation, 2012.

Coffman, D. J. and Hegg, D. A.: A preliminary study of the effect of ammonia on particle nucleation in the MBL, J. Geophys. Res., 100, 7147–7160, 1995.

Doyle, G. J.: Self-Nucleation in the Sulfuric Acid-Water System, J. Chem. Phys., 35, 795–799, 1961.

Erupe, M. E., Viggiano, A. A., and Lee, S.-H.: The effect of trimethylamine on atmospheric nucleation involving H_2SO_4, Atmos. Chem. Phys., 11, 4767–4775, doi:10.5194/acp-11-4767-2011, 2011.

Fuchs, N. A.: On the stationary charge distribution on aerosol particles in a bipolar ionic atmosphere, Geofis. Pura. Appl., 56, 185–193, 1963.

Ge, X., Wexler, A. S., and Clegg, S. L.: Atmospheric amines – Part I. A review, Atmos. Environ., 45, 524–546, 2011.

Hanson, D.: Mass accommodation of H_2SO_4 and CH_3SO_3H on water-sulfuric acid solutions from 6 to 97 % RH, J. Phys. Chem. A., 109, 6919–6927, doi:10.1021/jp0510443, 2005.

Hanson, D. R. and Eisele, F. L.: Diffusion of H_2SO_4 in humidified nitrogen: Hydrated H_2SO_4, J. Phys. Chem. A, 104, 1715–1719,

2000.

Hanson, D. R. and Eisele, F. L.: Measurement of prenucleation molecular clusters in the NH_3, H_2SO_4, H_2O system, J. Geophys. Res., 107, doi:10.1029/2001JD001100, 2002.

Hanson, D. R. and Kosciuch, E.: The NH_3 mass accommodation coefficient for uptake onto sulfuric acid solutions, J. Phys. Chem. A, 107, 2199–2208, 2003.

Hanson, D. R. and Lovejoy, E. R.: Measurement of the thermodynamics of the hydrated dimer and trimer of sulfuric acid, J. Phys. Chem. A, 110, 9525–9528, doi:10.1021/jp062844w, 2006.

Hanson, D. R., Eisele, F. L., Ball, S. M., and McMurry, P. M.: Sizing small sulfuric acid particles with an ultrafine particle condensation nucleus counter, Aerosol Sci. Tech., 36, 554–559, 2002.

Hanson, D. R, McMurry, P. H., Jiang, J., Tanner, D., and Huey, L. G.: Ambient Pressure Proton Transfer Mass Spectrometry: Detection of Amines and Ammonia, Environ. Sci. Technol., 45, 8881–8888, doi:10.1021/es201819a, 2011.

Hermann, E., Brus, D., Hyvärinen, A.-P., Stratmann, F., Wilck, M., Lihavainen, H., and Kulmala, M.: A Computational Fluid Dynamics Approach to Nucleation in the Water-Sulfuric Acid System, J. Phys. Chem. A, 114, 8033–8042, 2010.

IPCC: Fourth Assessment Report, Climate Change 2007: Working Group I: The Physical Science Basis, Technical Summary 2.2, Cambridge University Press, New York, USA available at: http://www.ipcc.ch/publications_and_data/ar4/wg1/en/tssts-2-2.html, 2007.

Kirkby, J., Curtius, J., Almeida, J., Dunne, E., Duplissy, J., Ehrhart, S., Franchin, A., Gagne, S., Ickes, L., Kurten, A., Kupc, A., Metzger, A., Riccobono, F., Rondo, L., Schobesberger, S., Tsagkogeorgas, G., Wimmer, D., Amorim, A., Bianchi, F., Breitenlechner, M., David, A., Dommen, J., Downard, A., Ehn, M., Flagan, R. C., Haider, S., Hansel, A., Hauser, D., Jud, W., Junninen, H., Kreissl, F., Kvashin, A., Laaksonen, A., Lehtipalo, K., Lima, J., Lovejoy, E. R., Makhmutov, V., Mathot, S., Mikkila, J., Minginette, P., Mogo, S., Nieminen, T., Onnela, A., Pereira, P., Petaja, T., Schnitzhofer, R., Seinfeld, J. H., Sipila, M., Stozhkov, Y., Stratmann, F., Tome, A., Vanhanen, J., Viisanen, Y., Vrtala, A., Wagner, P. E., Walther, H., Weingartner, E., Wex, H., Winkler, P. M., Carslaw, K. S., Worsnop, D. R., Baltensperger, U., and Kulmala, M.: Role of sulphuric acid, ammonia and galactic cosmic rays in atmospheric aerosol nucleation, Nature, 476, 429, doi:10.1038/nature10343, 2011.

Kuang, C.: Atmospheric nucleation: Measurements, mechanisms, and dynamics, in Department of Chemical Engineering and Materials Science, University of Minnesota, Minneapolis, 2009.

Kuang, C., Chen, M., McMurry, P. H., and Wang, J.: Optimization of laminar flow ultrafine condensation particle counters for the enhanced detection of 1 nm condensation nuclei, Aerosol Sci. Technol., 46, 309–315, doi:10.1080/02786826.2011.626815, 2012.

Kulmala, M., Vehkamäki, H., Petaja, T., Dal Maso, M., Lauri, A., Kerminen, V. M., Birmili, W., and McMurry, P. H.: Formation and growth rates of ultrafine atmospheric particles: a review of observations, J. Aerosol Sci., 35, 143–176, 2004.

Kurtén, T., Loukonen, V., Vehkamäki, H., and Kulmala, M.: Amines are likely to enhance neutral and ion-induced sulfuric acid-water nucleation in the atmosphere more effectively than ammonia, Atmos. Chem. Phys., 8, 4095–4103, doi:10.5194/acp-8-4095-2008, 2008.

Laaksonen, A., Talanquer, V., and Oxtoby, D.: Nucleation: Theory and atmospheric applications, Annu. Rev. Phys. Chem., 46, 489–524, 1995.

McGraw, R. and Wu, D. T.: Kinetic extensions of the nucleation theorem, J. Chem. Phys., 118, 9337–9347, 2003.

McMurry, P. H., Woo, K. S., Weber, R., Chen, D. R., and Pui, D. Y. H.: Size distributions of 3-10 nm atmospheric particles: implications for nucleation mechanisms, Phil. Trans. R. Soc. Lond. A, 358, 2625–2642, 2000.

Metzger, A., Verheggen, B., Dommen, J., Duplissy, J., Prevot, A. S. H., Weingartner, E., Riipinen, I., Kulmala, M., Spracklen, D. V., Carslaw, K. S., and Baltensperger, U.: Evidence for the role of organics in aerosol particle formation under atmospheric conditions, P. Natl. Acad. Sci., 107, 6646–6651, 2010.

Mirabel, P. and Ponche, J. L.: Studies of gas-phase clustering of water on sulphuric acid molecules, Chem. Phys. Lett., 183, 21–24, 1991.

Nel, A.: Air Pollution-Related Illness: Effects of Particles Science, Science, 308, 804–806, 2005.

Noppel, M.: Ethnalpy and entropy changes in formation of gas-phase sulfuric acid hydrates and dehydrates as a result of fitting to experimental pressure data, J. Geophys. Res., 105, 19779–19785, 2000.

Nowak, J. B., Huey, L. G., Russell, A. G., Tian, D., Neuman, J. A., Orsini, D., Sjostedt, S. J., Sullivan, A. P., Tanner, D. J., Weber, R. J., Nenes, A., Edgerton, E., and Fehsenfeld, F. C.: Analysis of urban gas phase ammonia measurements from the 2002 Atlanta Aerosol Nucleation and Real-Time Characterization Experiment (ANARChE), J. Geophys. Res, 111, D17308, doi:10.1029/2006JD007113, 2006.

Oberdorster, G., Ferin, J., Gelein, R., Soderholm, S. C., and Finkelstein, J.: Role of the alveolar macrophage in lung injury-Studies with ultrafine particles, Environ. Health Perspect., 97, 193–199, 1992.

O'Dowd, C. D., Aalto, P. P., Yoon, Y. J., and Hamerib, K.: The use of the pulse height analyser ultrafine condensation particle counter (PHA-UCPC) technique applied to sizing of nucleation mode particles of differing chemical composition, J. Aerosol Sci., 35, 205–216, 2004.

Oxtoby, D. W. and Kashchiev, D.: A general relation between the nucleation work and the size of the nucleus in multicomponent nucleation, J. Chem. Phys., 100, 7665–7671, 1994.

Panta, B., Glasoe, W. A., Zollner, J. A., Carlson, K. K., and Hanson, D. R.: Computational Fluid Dynamics of a Cylindrical Nucleation Flow Reactor with Detailed Cluster Thermodynamics, submitted to J. Phys. Chem. A, 2012.

Reiss, H.: The Kinetics of Phase Transitions in Binary Systems, J. Chem. Phys., 18, 840–848, 1950.

Saros, M. T., Weber, R. J., Marti, J. J., and McMurry, P. H.: Ultrafine aerosol measurement using a condensation nucleus counter with pulse height analysis, Aerosol Sci. Tech., 25, 200–213, 1996.

Sipilä, M., Berndt, T., Petäjä, T., Brus, D., Vanhanen, J., Stratmann, F., Patokoski, J., Mauldin III, R. L., Hyvärinen, A. P., Lihavainen, H., and Kulmala, M.: The role of sulfuric acid in atmospheric nucleation, Science, 327, 1243–1246, doi:10.1126/science.1180315, 2010.

Stoltzenburg, M. R. and McMurry, P. H.: An ultrafine aerosol condensation nucleus counter, Aerosol Sci. Technol., 14, 48–65, 1991.

Vehkamäki, H., Kulmala, M., Napari, I., Lehtinen, K. E. J., Timmreck, C., Noppel, M., and Laaksonen A.: An improved parameterization for sulfuric acid-water nucleation rates for tropospheric and stratospheric conditions, J. Geophys. Res., 107, 4622, doi:10.1029/2002JD002184, 2002.

Viisanen, Y., Kulmala, M., and Laaksonen, A.: Experiments on gas liquid nucleation of sulphuric acid and water, J. Chem. Phys., 107, 920–926, 1997.

Weber, R. J., McMurry, P. H., Mauldin, L., Tanner, D. J., Eisele, F. L., Brechtel, F. J., Kreidenweis, S. M., Kok, G. L., Schillawski, R. D., and Baumgardner, D.: A study of new particle formation and growth involving biogenic trace gas species measured during ace-1, J. Geophys. Res., 103, 16385–16396, 1998.

Weber, R. J., McMurry, P. H., Mauldin, R. L., Tanner, D. J., Eisele, F. L., Clarke, A. D., and Kapustin, V. N.: New particle formation in the remote troposphere: A comparison of observations at various sites, Geophys. Res. Lett., 26, 307–310, 1999.

Wyslouzil, B. E., Seinfeld, J. H., Flagan, R. C., and Okiuyama, K.: Binary nucleation in acid-water systems ii. Sulfuric acid-water and a comparison with methanesulfonic acid-water, J. Chem. Phys., 94, 6842–6850, 1991.

Yu, H., McGraw, R., and Lee, S. H.: Effects of amines on formation of sub-3 nm particles and their subsequent growth, Geophys. Res. Lett., 39, L02807, doi:10.1029/2011GL050099, 2012.

Young, L. H., Benson, D. R., Kameel, F. R., Pierce, J. R., Junninen, H., Kulmala, M., and Lee, S.-H.: Laboratory studies of H_2SO_4/H_2O binary homogeneous nucleation from the SO_2+OH reaction: evaluation of the experimental setup and preliminary results, Atmos. Chem. Phys., 8, 4997–5016, doi:10.5194/acp-8-4997-2008, 2008.

Zhang, R. H., Suh, I., Zhao, J., Zhang, D., Fortner, E. C., Tie, X., Molina, L. T., and Molina, M. J.: Atmospheric new particle formation enhanced by organic acids, Science, 304, 1487–1490, 2004.